hep-th/0502127

Topology Changing Transitions in Bubbling Geometries

Petr Hořava and Peter G. Shepard

Berkeley Center for Theoretical Physics and Department of Physics
University of California, Berkeley, CA 94720-7300
and
Theoretical Physics Group, Lawrence Berkeley National Laboratory
Berkeley, CA 94720-8162, USA
horava, pgs@socrates.berkeley.edu

Abstract

Topological transitions in bubbling half-BPS Type IIB geometries with $SO(4) \times SO(4)$ symmetry can be decomposed into a sequence of n elementary transitions. The half-BPS solution that describes the elementary transition is seeded by a phase space distribution of fermions filling two diagonal quadrants. We study the geometry of this solution in some detail. We show that this solution can be interpreted as a time dependent geometry, interpolating between two asymptotic pp-waves in the far past and the far future. The singular solution at the transition can be resolved in two different ways, related by the particle-hole duality in the effective fermion description. Some universal features of the topology change are governed by two-dimensional Type 0B string theory, whose double scaling limit corresponds to the Penrose limit of $AdS_5 \times S^5$ at topological transition. In addition, we present the full class of geometries describing the vicinity of the most general localized classical singularity that can occur in this class of half-BPS bubbling geometries.

February 2005

1. Introduction

An intriguing picture of half-BPS geometries of Type IIB string theory corresponding to the chiral primaries (with $\Delta = J$) of $\mathcal{N} = 4$ SYM theory has emerged recently in the work of Lin, Lunin and Maldacena (LLM) [1]. In this picture, the data defining the geometry is captured by a distribution of incompressible droplets of fermions on a $1 + 1$ dimensional phase space. Since the effective $\hbar$ of the fermions is related to the Planck length of Type IIB supergravity via $\hbar = 2\pi\ell_p^4$, the semiclassical limit of the Fermi system – in which it makes sense to talk about the geometry of the Fermi surface in phase space – corresponds to the semiclassical limit of the Type IIB geometry. On the CFT side, the fermionic picture of the geometries nicely matches the fermions emerging as the eigenvalues in the gauged matrix model description of the corresponding half-BPS states with $\Delta = J$ (schematically of the form $\Pi_i \mathrm{Tr}(Z^{n_i})^{r_i}$), in the harmonic oscillator potential [2-5] (see also [6]).

Generically, an individual classical geometry corresponds to some distribution of fermions with a number of boundaries between occupied and unoccupied regions. Zooming in on a small part of the boundary between the two regions corresponds to a pp-wave limit of the geometry, and thus the geometry is nonsingular in the vicinity of such boundary.

As we move around in the moduli space of such geometries, the phase space liquid will flow while preserving its total area. In the process, the number of components of the Fermi surface separating the filled and empty regions can change. In the corresponding Type IIB geometry, this represents a spacetime topology change.

Generically, this change will happen by two boundaries approaching each other and reconnecting with a net change of boundary components by ± 1 (see Fig. 1).

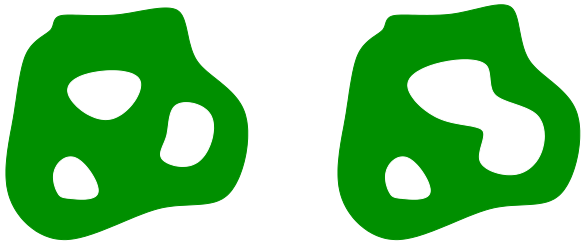

Fig. 1: Two semiclassical phase space distributions of fermions, related by a topological transition that changes the number of components of the Fermi surface by ± 1.

More complicated topology changing processes in bubbling geometries are also possible: for example, one can envision more than two boudary components meeting and reconnecting. However, since the phase space of the fermions is only two-dimensional, any

such process is non-generic and can be smoothly deformed into a sequence of steps, each step only involving the elementary process of two boundaries reconnecting.[1]

We wish to understand the geometry at the transition when two boundary components meet and reconnect. The universal features of the transition will be captured by the local region where the two boundary components touch. We will isolate these universal features by zooming in on the intersection. The fermions that source this geometry occupy two opposite infinite quadrants on phase space, as in Fig. 2.[2] All other topology changing processes in the bubbling Type IIB geometries of LLM are then decomposable into n steps, each involving the unique topology changing process studied here.

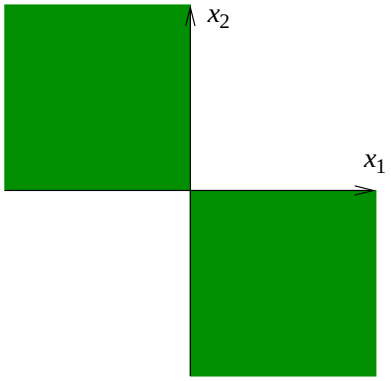

Fig. 2: The phase space distribution of fermions that seeds the universal part of the geometry at the topological transition.

This paper is organized as follows. In Section 2, we present the univesal topology changing solution and study some of its properties. In Section 3 we reinterpret this solution as a time-dependent process. In Section 4 we study resolutions to non-singular geometries with the same asymptotic behavior; here the non-critical $\hat{c} = 1$ Type 0B strings make an appearance. In Section 5 we embed the topology changing process into $AdS_5 \times S^5$, refining our understanding of how the universal properties of the topology change are captured by the double scaling limit known to define the noncritical Type 0B string theory in two dimensions. In Section 6 we consider the complete class of half-BPS LLM geometries of Type IIB theory with the additional property of scaling; these geometries describe the most general composite classical singularities that can occur in the "quantum-foam" topological transitions in LLM geometries.

[1] A full class of non-generic localized topology changing processes is discussed in Section 6.

[2] For simplicity, we shall concentrate on the case of Fermi surface components meeting at right angles throughout most of the paper, relegating the more general case of arbitrary angles to Section 6.

2. The Half-BPS Solution at Topological Transition

2.1. LLM geometries

It has been shown in [1] that the most general half-BPS solution of Type IIB supergravity with $SO(4) \times SO(4) \times \mathbf{R}$ symmetry, with only the metric and the five-form RR flux excited, can be written as

$$ds^2 = -h^{-2}(dt + V_i dx^i)^2 + h^2(dy^2 + dx^i dx^i) + R^2 d\Omega_3^2 + \widetilde{R}^2 d\widetilde{\Omega}_3^2 \tag{2.1}$$

and

$$F_5 \equiv F_{\mu\nu} dx^\mu \wedge dx^\nu \wedge d\Omega_3 + \widetilde{F}_{\mu\nu} dx^\mu \wedge dx^\nu \wedge d\widetilde{\Omega}_3, \tag{2.2}$$

with the two two-forms $F_{\mu\nu}$ and $\widetilde{F}_{\mu\nu}$ given by

$$\begin{aligned} F &= -\frac{1}{4}\left\{ d\left(R^4(dt+V)\right) + y^3 *_3 d\left(\frac{z+\frac{1}{2}}{y^2}\right)\right\}, \\ \widetilde{F} &= -\frac{1}{4}\left\{ d\left(\widetilde{R}^4(dt+V)\right) + y^3 *_3 d\left(\frac{z-\frac{1}{2}}{y^2}\right)\right\}. \end{aligned} \tag{2.3}$$

Here R and $\widetilde{R}$ are the radii of the two three-spheres on which the two $SO(4)$'s act transitively (following [1], we shall denote them simply by S^3 and $\widetilde{S}^3$), and t corresponds to the time coordinate with $\partial/\partial t$ the (mostly timelike) Killing vector that generates the $\mathbf{R}$ part of the symmetry group. In Eqn. (2.2) for the fluxes, x^μ with $\mu = 0, \ldots 3$ refers collectively to the four coordinates t, x_i, y, and $*_3$ is the Hodge operator on the x_i, y space with respect to its flat metric.

All the coefficients $R, \widetilde{R}, V_1, V_2$ and h in (2.1) are determined in terms of a single function z on the three-dimensional space x_1, x_2, y. The radii R and $\widetilde{R}$ of the S^3 and $\widetilde{S}^3$ factors of the geometry are given in terms of z by

$$R^2 = y\sqrt{\frac{1+2z}{1-2z}}, \qquad \widetilde{R}^2 = y\sqrt{\frac{1-2z}{1+2z}}, \tag{2.4}$$

the coefficient h is given by

$$h^{-2} = \frac{2y}{\sqrt{1-4z^2}} = R^2 + \widetilde{R}^2, \tag{2.5}$$

and the components of V can be determined, once z is known, from

$$y\partial_y V_i = \epsilon_{ij}\partial_j z, \qquad y(\partial_i V_j - \partial_j V_i) = \epsilon_{ij}\partial_y z. \tag{2.6}$$

The equations of motion of Type IIB supergravity are then equivalent to the following linear equation for the function z,

$$\partial_i \partial_i z + y\partial_y\left(\frac{\partial_y z}{y}\right) = 0, \tag{2.7}$$

where $\partial_i \partial_i$ is the flat-space Laplacian on the (x_1, x_2) plane. Since $y = R\widetilde{R}$, y takes only positive values, and (2.7) can be solved by first selecting an initial condition $z(x_1, x_2, 0)$ and then solving for the y dependence of z by (2.7). The initial condition on z at $y = 0$ can be a priori arbitrary, but unless $z(y = 0)$ is only equal to $\pm 1/2$ the geometry is singular. Thus, all solutions of the LLM type are classified by specifying the areas on the x_1, x_2 plane where z is $1/2$ or $-1/2$; by reinterpreting these two regions as being empty or filled by semiclassical fermions, one can establish the correspondence between such half-BPS geometries and the corresponding half-BPS operators in the CFT dual (reduced to the matrix model).

As an example, $AdS_5 \times S^5$ itself corresponds to the circular Fermi surface. Its Penrose limit corresponds to the Fermi sea filling one half of the phase space, with a linear Fermi surface; this is the Fermi description of the Type IIB pp-wave. In both of these special examples, the Fermi sea develops an "accidental" extra symmetry compatible with the flat metric on the (x_1, x_2) plane: rotations around the origin in the case of $AdS_5 \times S^5$, or translations along the Fermi surface for the pp-wave. In the full geometry, these extra symmetries give rise to additional Killing vectors.

Conversely, one can interpret individual Killing vectors of the full Type IIB geometry in terms of flows on the phase space of the Fermi system: for example, the generator $H \equiv \Delta$ of time translations in the conventional global coordinates on $AdS_5 \times S_5$ corresponds to the Hamiltonian flow that uniformly rotates the phase space around the center of the Fermi sea. All geometries have at least one Hamiltonian flow associated with the Killing vector mandated by the presence of supersymmetry; in the terminology of the CFT dual, this Hamiltonian flow is generated by $H' = \Delta - J$, and acts trivially on the x_1, x_2 plane.

2.2. The solution at topological transition in LLM coordinates

After this brief summary of the results of [1], we can introduce the solution that captures the universal features of the unique generic topology-changing process in all half-BPS Type IIB geometries of this class. As discussed in the Introduction, this leads us to solve for z sourced by fermions distributed in two opposite infinite quadrants (cf. Fig. 2),

$$z(x_1, x_2, 0) = \frac{1}{2} \operatorname{sign}(x_1) \operatorname{sign}(x_2). \tag{2.8}$$

The solution of (2.7) with such initial conditions is

$$z(x_1, x_2, y) = \frac{x_1}{\pi \sqrt{x_1^2 + y^2}} \arctan\left(\frac{x_2}{\sqrt{x_1^2 + y^2}}\right) + \frac{x_2}{\pi \sqrt{x_2^2 + y^2}} \arctan\left(\frac{x_1}{\sqrt{x_2^2 + y^2}}\right). \tag{2.9}$$

Given this z, one can also find the components of the vector field V,

$$\begin{aligned} V_1(x_1, x_2, y) &= -\frac{1}{\pi\sqrt{x_2^2+y^2}} \arctan\left(\frac{x_1}{\sqrt{x_2^2+y^2}}\right), \\ V_2(x_1, x_2, y) &= \frac{1}{\pi\sqrt{x_1^2+y^2}} \arctan\left(\frac{x_2}{\sqrt{x_1^2+y^2}}\right). \end{aligned} \tag{2.10}$$

Having determined V, one can – in retrospect – write z in the following simple form,

$$z(x_1, x_2, y) = x_1 V_2 - x_2 V_1. \tag{2.11}$$

The rest of the geometry, including the RR five-form fluxes, is then known in terms of z as summarized in the previous subsection.

Since one of the requirements in the construction of all LLM solutions is the existence of a sixteen-component generalized Killing spinor, our solution is guaranteed to have (at least) sixteen supersymmetries.

2.3. Scaling properties

Since the phase space distribution of the fermions that seeds this geometry is scale invariant, the metric will inherit an interesting scaling property. Consider the following transformation,

$$x_i \to \lambda x_i, \qquad y \to \lambda y. \tag{2.12}$$

Under this tranformation, we have

$$\begin{aligned} z \to z, \qquad & V_i \to \lambda^{-1} V_i, \\ R \to \lambda^{1/2} R, \qquad & \widetilde{R} \to \lambda^{1/2} \widetilde{R}, \\ h \to & \lambda^{-1/2} h. \end{aligned} \tag{2.13}$$

In particular, z is invariant under this scaling transformation.

If we now extend the action of our scaling transformation to t and the six angle coordinates on S^3 and $\widetilde{S}^3$ so that they are all scaling invariant,

$$t \to t, \qquad d\Omega_3^2 \to d\Omega_3^2, \qquad d\widetilde{\Omega}_3^2 \to d\widetilde{\Omega}_3^2, \tag{2.14}$$

the metric and the RR flux will transform as follows,

$$ds^2 \to \lambda ds^2, \qquad F_5 \to \lambda^2 F_5. \tag{2.15}$$

In Section 6 we will study a complete class of solutions which share the same scaling property.

2.4. Behavior near $y = 0$

Consider the nine-dimensional slice $\mathcal{M}_9$ of constant t in our solution at topological transition, as given by (2.9), (2.10), (2.1) and (2.2). Away from the $y = 0$ hypersurface, the product of the two three-spheres $S^3 \times \widetilde{S}^3$ is trivially fibered over the topologically trivial open domain (x_1, x_2, y), $y > 0$. In order to understand various properties of $\mathcal{M}_9$, such as its global topology, we first need to determine the behavior at $y = 0$. The radii of the two spheres are given by $y\sqrt{\frac{1\pm 2z}{1\mp 2z}}$, Eqn. (2.4). When we approach $y = 0$, z approaches $\pm 1/2$. In this limit, one of the radii will always go to zero, while the other one will generically stay finite. In the case of our solution, the radius of the first S^3 is non-zero in the two quadrants where $\mathrm{sign}\,(x_1/x_2) = 1$, and its value there is

$$R^2(y=0) = (2\pi|x_1x_2|)^{1/2}\left(1 + \frac{x_1}{x_2}\arctan\left(\frac{x_1}{x_2}\right) + \frac{x_2}{x_1}\arctan\left(\frac{x_2}{x_1}\right)\right)^{-1/2}. \qquad (2.16)$$

Similarly, the radius of $\widetilde{S}^3$ is also given by (2.16), but now in the complementary quadrants satisfying $\mathrm{sign}\,(x_1/x_2) = -1$. At the boundary between the two regions, both spheres shrink to zero volume, and the geometry is smooth everywhere outside of $x_i = y = 0$.

Having calculated the radii of S^3 and $\widetilde{S}^3$ at $y = 0$, we can now examine the norm of the "mandatory" Killing vector $\partial/\partial t$ whose existence follows from the BPS property of the solution,

$$\begin{aligned}\left\|\frac{\partial}{\partial t}\right\|^2 &= -R^2 - \widetilde{R}^2 \\ &= -(2\pi|x_1x_2|)^{1/2}\left(1 + \frac{x_1}{x_2}\arctan\left(\frac{x_1}{x_2}\right) + \frac{x_2}{x_1}\arctan\left(\frac{x_2}{x_1}\right)\right)^{-1/2}.\end{aligned} \qquad (2.17)$$

This formula is valid everywhere on the (x_1, x_2) plane at $y = 0$. Thus, the Killing vector $\partial/\partial t$ is time-like inside the $z = \pm 1/2$ regions, and turns null at the boundaries between the regions. In particular, the singularity at the origin is a null singularity. Since the radii of both S^3 and $\widetilde{S}^3$ shrink to zero there, the singularity corresponds in the full ten-dimensional geometry to a null worldline of a point-like massless particle. Outside of the $y = 0$ hypersurface, both R and $\widetilde{R}$ are non-zero, and $\partial/\partial t$ is strictly timelike.

2.5. The topology of the solution

In order to determine the global topology of $\mathcal{M}_9$, we shall now study eight-dimensional closed surfaces inside $\mathcal{M}_9$, constructed by fibering $S^3 \times \widetilde{S}^3$ over a two-dimensional disk Σ_D embedded into the x_1, x_2, y space such that $\partial\Sigma_D$ is inside the $y = 0$ surface, while the interior of Σ_D is mapped into the region with $y > 0$.

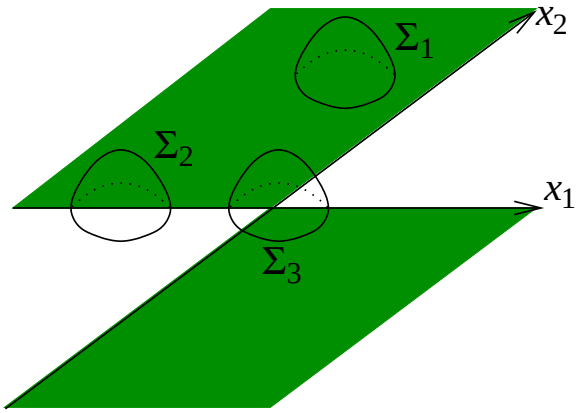

Fig. 3: The three eight-surfaces discussed in Section 2.5. The surfaces obtained from the disks Σ_1, Σ_2 and Σ_3 are topologically $S^5 \times S^3$, S^8 and $S^4 \times S^4$, respectively.

There are three interesting cases to consider. They correspond to $\Sigma_D = \Sigma_1, \Sigma_2$ and Σ_3 in Fig. 3.

If $\partial\Sigma_D$ lies entirely within the filled or empty region (as is the case for $\Sigma_D = \Sigma_1$ of Fig. 3), one of the three-spheres shrinks to zero volume uniformly along $\partial\Sigma_D$ while the other S^3 stays at non-zero volume – the resulting eight-surface is topologically $S^5 \times S^3$ or $S^3 \times S^5$.

If $\partial\Sigma_D$ intersects a smooth boundary component between the filled and empty region in two points (cf. Σ_2 in Fig. 3), the resulting surface has the topology of S^8. This can be seen for example by first foliating Σ_D by one-dimensional compact intervals I such that one end-point of I lies on $\partial\Sigma_D$ inside the filled region while the other end-point lies on $\partial\Sigma_D$ inside the empty region. Over I, one S^3 shrinks to zero volume at one end-point of I, while the other S^3 shrinks to zero volume at the other end-point of I. Hence, I together with the two three-spheres form an S^7. The total eight-surface costructred from S^3 and $\widetilde{S}^3$ over Σ_D is then a foliation of S^8 by S^7's whose volume shrinks to zero at the two poles of S^8 where the surface intersects the boundary between the filled and empty region on the (x_1, x_2) plane at $y = 0$.

Finally, when $\partial\Sigma_D$ encircles the singular point at the origin, hence intersecting the boundary between the filled and empty regions in four points, the resulting surface is $S^4 \times S^4$. This can be again demonstrated by an argument similar to the one used in the previous paragraph. The boundary $\partial\Sigma_D$ of the disk is now divided into four segments; inside each segment, one S^3 has non-zero volume while the other one has shrunk to a point. The two S^3's exchange their roles as we move from segment to segment along $\partial\Sigma_D$. Imagine cutting the disk Σ_D along a line connecting two boundary points on the two opposite segments of the boudary where the same S^3 has non-zero volume. This cut splits the eight-manifold that results from fibefing the two S^3 over Σ_D into two open eight-

manifolds. These open eight-manifolds are each topologically $D_4 \times S^4$, and they are glued together along their $S^3 \times S^4$ boundary so as to form $S^4 \times S^4$. The two noncontractible S^4 cycles on this surface are given by the four-manifolds obtained from considering one of the boundary segments on $\partial\Sigma_D$ and fibering the S^3 of non-zero volume over it.

The scaling property of our metric then implies that the full topology of the surfaces $\mathcal{M}_9$ of constant t in our solution is that of a cone over $S^4 \times S^4$. While the metric outside of the tip of the cone is smooth, there is a singularity at the tip of the cone at $x_i = y = 0$.

2.6. Asymptotics to pp-waves

There are regimes where our geometry approaches that of a pp-wave. Indeed, consider the metric in the limit where (say) $x_1 \gg |x_2|, |y|$. In that limit, we obtain

$$z(x_1, x_2, y) \approx \frac{x_2}{2\sqrt{x_2^2 + y^2}} \quad + \mathcal{O}\left(x_2/x_1, y/x_1\right), \tag{2.18}$$

and

$$\begin{aligned} V_1 &\approx -\frac{1}{2\sqrt{x_2^2 + y^2}} \quad + \mathcal{O}\left(\sqrt{x_2^2 + y^2}/x_1\right), \\ V_2 &\approx \quad 0 + \mathcal{O}\left(x_2/x_1, y/x_1\right), \end{aligned} \tag{2.19}$$

(and similarly for the rest of the geometry including the RR fluxes.) This is the maximally symmetric pp-wave solution of Type IIB theory, rewritten in the LLM coordinates. The standard form of the pp-wave geometry is obtained by introducing coordinates

$$r_1 = R = \sqrt{x_2 + \sqrt{x_2^2 + y^2}}, \qquad r_2 = \widetilde{R} = \sqrt{-x_2 + \sqrt{x_2^2 + y^2}}, \tag{2.20}$$

and x_1. In these coordinates, the metric becomes

$$\begin{aligned} ds^2 = -2dtdx_1 - (r_1^2 + r_2^2)dt^2 + dr_1^2 + r_1^2 d\Omega_3^2 + dr_2^2 + r_2^2 d\widetilde{\Omega}_3^2 \\ + \mathcal{O}(r_1^2/x_1, r_2^2/x_1). \end{aligned} \tag{2.21}$$

Notice that in this asymptotic pp-wave regime, $\partial/\partial x_1$ becomes an asymptotic Killing vector.

Similarly, we could have considered any of the four regimes $\pm x_1 \gg |x_2|, |y|$ or $\pm x_2 \gg |x_1|, |y|$; in each of these regimes, our geometry is asymptotic to a pp-wave. As a result of this asymptotic behavior, our solution develops extra asymptotic Killing symmetries and supersymmetries in these asymptotic regions.

3. The Geometry at Topological Transition as a Time-Dependent Process

Until now we studied the solution in the LLM coordinates, in which it is manifestly stationary. These coordinates are natural from the point of view of observers following the orbits of the (mostly) timelike Killing vector $K \equiv \partial/\partial t$. This Killing vector indeed plays a crucial role in the LLM geometries, since it corresponds to $H' = \Delta - J$ on the CFT side, and supercharges square to K.

We will now show that in our topology-changing geometry, a different class of natural observers can be introduced, for which the geometry asymptotes to a more conventional pp-wave geometry in the far past and the far future, and appears time-dependent at intermediate times.

The fact that different observers can perceive a given geometry differently is indeed one of the crucial features of quantum gravity. Making sense of the observations of the same geometry by different observers is one of the most intriguing challenges in cases such as de Sitter space or the Schwarzschild black hole. Our hope is that addressing such questions first in the more controlled case of supersymmetric geometries (such as those studied in this paper) might lead to important lessons with a broader range of applicability.

3.1. Relation to pp-waves

As we showed in Section 2.6, our solution is asymptotic to the maximally supersymmetric Type IIB pp-wave, in the four regimes where $|x_1|$ or $|x_2|$ is much larger than the other coordinates on the x_i, y space. We now introduce a new coordinate system, replacing x^μ with

$$\begin{aligned} t &= t', \\ y &= r_1 r_2, \\ x_2 &= \frac{1}{2}(r_1^2 - r_2^2), \\ x_1 &= w + t'. \end{aligned} \tag{3.1}$$

These coordinates have been designed such that, asymptotically in the far past $t' \to -\infty$, our solution is asymptotic to the maximally supersymmetric pp-wave. Thus, at early times in this coordinate system, we have

$$\begin{aligned} ds^2 \approx -2dt'dw - [2 + r_1^2 + r_2^2]dt'^2 + dr_1^2 + r_1^2 d\Omega_3^2 + dr_2^2 + r_2^2 d\widetilde{\Omega}_3^2 \\ + \mathcal{O}(r_1^2/t', r_2^2/t', w/t'). \end{aligned} \tag{3.2}$$

The (noninertial) observers who are static with respect to this coordinate system will follow the lines of

$$\frac{\partial}{\partial t'} = \frac{\partial}{\partial t} + \frac{\partial}{\partial x_1}. \tag{3.3}$$

In the asymptotic regime $t' \to -\infty$, becomes a Killing vector. However, since $\partial/\partial x_1$ is a Killing vector only asymptotically as $x_1 \to -\infty$, $\partial/\partial t'$ will not be a Killing vector at finite t': the observers will see a time-dependent geometry. In the far past, such observers start in one of the asymptotic, asymptotically stationary pp-wave regimes, $x_1 \to -\infty$.

We can similarly define observers who see a geometry that asymptotes to a pp-wave in their far future. Introduce coordinates similar to those in (3.1),

$$\begin{aligned} t &= t', \\ y &= r_1 r_2, \\ x_1 &= \frac{1}{2}(r_1^2 - r_2^2), \\ x_2 &= w - t'. \end{aligned} \tag{3.4}$$

The observers who follow $\partial/\partial t'$ in these coordinates will end up in the pp-wave asymptotic regime $x_2 \to \infty$ at late times, $t' \to \infty$.

The observers introduced in this subsection see our topology-changing half-BPS solution quite differently from the stationary observers who follow the worldlines of the Killing vector K. From their perspective, the geometry is more naturally interpreted as a time-dependent, background-scattering process, with a well-defined in- and out- asymptotics given by the maximally supersymmetric pp-wave. It would be natural for such observers to probe the geometry by weakly interacting probes.[3] The natural in-states and out-states are the excitations of the pp-wave geometry, and the natural observables are S-matrix-like elements (or reflection/transmission coefficients) for the scattering of such quanta off of the time-dependent geometry. The high degree of solvability of string theory in the asymptotic regimes, and the fact that our solution is half-BPS, suggest that a much more detailed analysis should be possible. This is, however, outside of the scope of this paper.

3.2. Matching the asymptotic pp-wave regimes

The time-dependent interpretation of our solution takes advantage of the pp-wave asymptotics, but it does so only in one pp-wave regime at a time. For example, the coordinate system (3.1) is really natural at early times, but becomes less well-behaved at late times. A different coordinate system, capable of capturing all four asymptotic pp-wave regimes, would be desirable.

In order to motivate such a coordinate system, note first that the Fermi surface that seeds our geometry satisfies a simple equation $x_1 x_2 = 0$. This can be considered a limit as $\mu \to 0$ of a smooth, hyperbolic Fermi surface $x_1 x_2 = \mu$, a fact that will take further

[3] In particular, if such probes are to maintain the half-BPS property of the geometry, they will be mutually non-interacting.

advantage of in the next section. This entire family of Fermi surfaces enjoys an extra symmetry, suggesting the possibility of following a hyperbolic-type flow. Such a flow will interpolate between the far-past and the far-future pp-wave asymptotics.

The most straigthforward hyperbolic flow – following the lines of constant $x_1 x_2$ – would not be a suitable choice, however. This flow does interpolate bewteen the regions of $x_1 \gg x_2$ and $x_2 \gg x_1$, but it does not produce a regular coordinate system in the asymptotic limit. However, there is a natural "regularization" of the hyperbolic flow, which is in fact encoded in the geometry of our solution. Consider the one-form $V = V_i dx^i$ that appears in the metric. The corresponding dual vector $\hat{V}$ is given by

$$\hat{V} = h^{-2} \left(V_i \frac{\partial}{\partial x_i} - (V_i V_i) \frac{\partial}{\partial t} \right). \tag{3.5}$$

We will denote by $\widetilde{V}$ the projection of $\hat{V}$ onto the surfaces of constant t. The flow of $\widetilde{V}$ on the x_1, x_2 plane (cf. Fig. 4) has exactly the properties we look for:

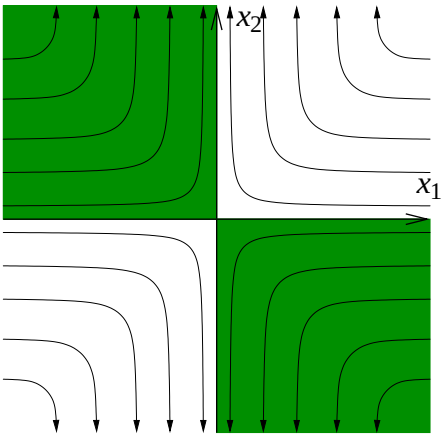

Fig. 4: The flow of $\widetilde{V}$ on the (x_1, x_2) plane at $y = 0$ in the LLM coordinates.

(1) The flow of $\widetilde{V}$ interpolates between the asymptotic regions with large $|x_1|$ in the far past and the asymptotic regions with large $|x_2|$ in the far future,

(2) $\widetilde{V}$ approaches the asymptotic Killing vectors in the corresponding asymptotic regions; for example,

$$\widetilde{V} \approx -\frac{\partial}{\partial x_1} \qquad \text{for } x_1 \to \infty. \tag{3.6}$$

These observations suggest a particularly natural coordinate system to interpolate between the time-dependent interpretations of the solution in the four asymptotic pp-wave regimes. Instead of following the lines of constant x_1 or x_2, the observers follow the regulated hyperbolic flow lines of $\widetilde{V}$. In such coordinates, the geometry is time dependent, and interpolates between two widely separated pp-waves (regimes of $|x_1| \to \infty$) in the

asymptotic past, and two widely separated pp-waves (regimes with $|x_2| \to \infty$) in the asymptotic future. This picture again suggests that a natural interpretation of our solution is in terms of a scattering process.

4. Resolutions

Until now we studied the half-BPS solution directly at the point of the topological transition. This solution has a null point-like singularity at the origin, and the hypersurfaces of constant t are topologically isomorphic copies of a cone over $S^4 \times S^4$. In this section, we will study the smooth resolutions of this singularity, within the family of half-BPS LLM geometries. In the language of the fermions, such resolutions are simply accomplished by separating the Fermi surface into two smooth, disconnected components (cf. Fig. 5). This can be done in two ways, leading to a one-parameter family of solutions interpolating between the two resolutions, and capturing the unique elementary topology change in this class of Type IIB geometries.

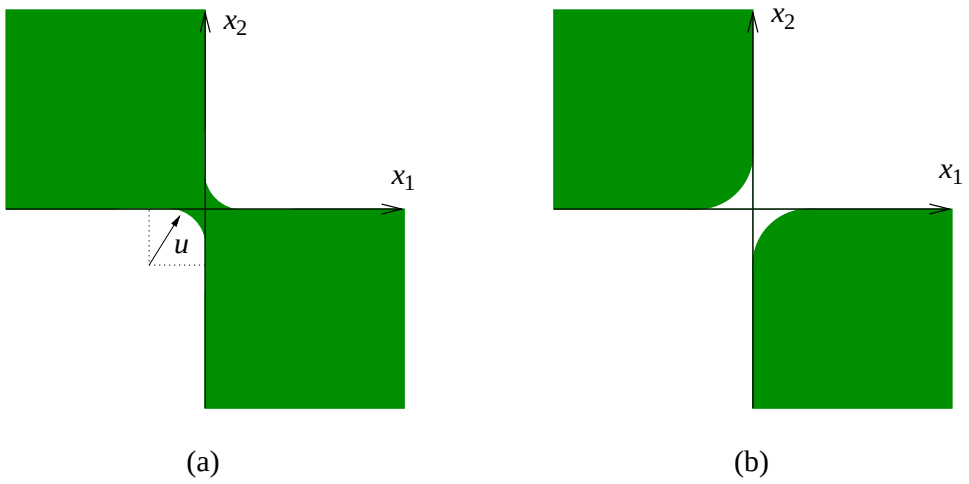

Fig. 5: The transition geometry can be resolved in two ways, related to each other by the particle-hole duality in the fermion picture.

4.1. A one-parameter family of resolved geometries

First we will consider a typical resolved geometry, for which the Fermi surface is affected only in some compact region of size u around the origin. For concreteness, we pick the distribution of fermions whose Fermi surface is given by $(x_1 - u)^2 + (x_2 - u)^2 = u^2$ for $0 \leq x_1, x_2 \leq u$, $(x_1 + u)^2 + (x_2 + u)^2 = u^2$ for $-u \leq x_1, x_2 \leq 0$, and by $x_1 x_2 = 0$ otherwise (Fig. 5(a)). The positive parameter $u > 0$ is a modulus of this family of solutions.

The corresponding function z seeded by this distribution of fermions can be analytically evaluated, leading to

$$\begin{aligned} z(x_1,x_2,y) = & \frac{x_1}{2\pi\sqrt{x_1^2+y^2}}\arctan\left(\frac{x_2-u}{\sqrt{x_1^2+y^2}}\right)+\frac{x_2}{2\pi\sqrt{x_2^2+y^2}}\arctan\left(\frac{x_1-u}{\sqrt{x_2^2+y^2}}\right) \\ & +\frac{1}{4}+\frac{x_1}{2\pi\sqrt{x_1^2+y^2}}\arctan\left(\frac{x_2+u}{\sqrt{x_1^2+y^2}}\right)+\frac{x_2}{2\pi\sqrt{x_2^2+y^2}}\arctan\left(\frac{x_1+u}{\sqrt{x_2^2+y^2}}\right) \\ & -\frac{H_-}{2\pi\sqrt{H_-^2+4u^2y^2}}\left\{\arctan\left(\frac{\sqrt{H_-^2+4u^2y^2}}{x_1^2+x_2^2+y^2-u^2}\right)+\frac{\pi}{2}\left[1-\ \mathrm{sign}\,(x_1^2+x_2^2+y^2-u^2)\right]\right\} \\ & -\frac{H_+}{2\pi\sqrt{H_+^2+4u^2y^2}}\left\{\arctan\left(\frac{\sqrt{H_+^2+4u^2y^2}}{x_1^2+x_2^2+y^2-u^2}\right)+\frac{\pi}{2}\left[1-\ \mathrm{sign}\,(x_1^2+x_2^2+y^2-u^2)\right]\right\} \end{aligned} \tag{4.1}$$

where we have introduced a shorthand notation

$$H_\pm = (x_1 \pm u)^2 + (x_2 \pm u)^2 + y^2 - u^2. \tag{4.2}$$

The family that corresponds to Fig. 5(b) can be obtained from (4.1) by rotating the phase space by $\pi/2$ and invoking the particle-hole duality. We will parametrize this other branch of resolved geometries by negative values of u, with $-u$ being the size of the resolved region in Fig. 5(b). Interpolating between positive and negative u takes the geometry through the topology changing transition.

The analytic form of this class of half-BPS solutions in the LLM coordinates is admittedly not too illuminating, besides illustrating that (a) a family can be analytically constructed, and (b) that the generic solution in the LLM class is fairly complicated (at least in the LLM coordinates).

Having resolved the singular geometry in two different ways, we can now analyze in more detail the change of topology that this entails as u is varied. At $u \neq 0$, the geometry is non-singular. As we approach $u = 0$, the topology of the spatial sections changes, from $R^5 \times S^4$ at $u < 0$, via the cone over $S^4 \times S^4$ at $u = 0$, to $S^4 \times R^5$ at $u > 0$. During this process of topology change, an S^4 cycle in $R^5 \times S^4$ shrinks to a point (say) at the origin of R^5, thus forming a singular cone over $S^4 \times S^4$ at $u > 0$. Then the singular point blows up into another S^4, turning the topology of the solution into the nonsingular $S^4 \times R^5$. In the process, the contractible and non-contractible factors of the geometry exchanged their roles. This mechanism of topology changing transition is notably reminiscent of the behavior near the conifold singularities of Calabi-Yau manifolds.

4.2. Resolutions and two-dimensional Type 0B strings

The particular details of how the Fermi surface is separated into two disconnected

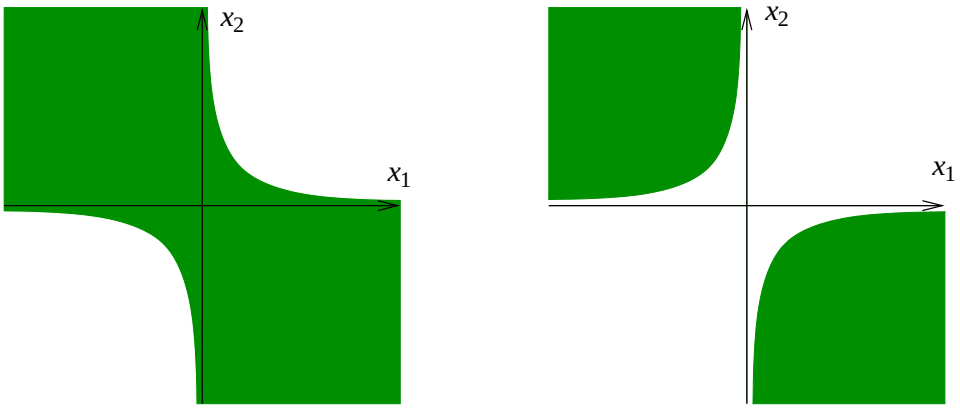

Fig. 6: The resolution that corresponds to the Fermi surface of non-critical $\hat{c} = 1$ Type 0B string theory.

smooth components are immaterial: any such resolved distribution of fermions will give rise to a non-singular Type IIB geometry whose topology is as described above. Two resolutions that differ from each other just by a ripple on the Fermi surface are related to each other by excitations of the supergravity modes on this background.

Consider a distribution of fermions such that the Fermi surface is given by

$$x_1 x_2 = 2\mu, \tag{4.3}$$

where positive and negative values of μ correspond to Fig. 6(a) and 6(b) respectively. When $\mu = 0$ we recover our original geometry, while for $\mu \neq 0$ this represents another one-parameter family of smooth solutions undergoing the topology change as $\mu \to 0$. This family is topologically equivalent to the one constructed in the previous subsection, since their corresponding fermion distributions differ only by a wave on the Fermi surface.

After a simple redefinition of coordinates,

$$p = \frac{1}{\sqrt{2}}(x_1 + x_2), \qquad q = \frac{1}{\sqrt{2}}(x_1 - x_2). \tag{4.4}$$

the Fermi surface (4.3) can be written as

$$p^2 - q^2 = \mu. \tag{4.5}$$

This is the Fermi surface of the much studied two-dimensional non-critical string theory (see [7] for reviews), in the canonical phase space coordinates. In fact, since both sides of the Fermi sea are filled, this is more precisely interpreted as the Fermi sea of the ground state of the $\hat{c} = 1$ Type 0B string theory, as described by the matrix model with the inverted harmonic oscillator potential [8].

Noncritical string theory has appeared in the description of critical string backgrounds near singularities before (see, e.g., [9-12]). In our case, it is the full Type 0B theory in two dimensions with uncompactified, Lorentz-signature time that makes its appearance, not just the topological or Euclidean version of this noncritical string theory.

This appearance of the Fermi surface of the inverted harmonic oscillator in the description of the half-BPS Type IIB geometry near its topological transition can be naturally interpreted on the CFT side of the AdS/CFT correspondence as follows. In CFT, the half-BPS operators with $\Delta = J$ are described by the gauged matrix model [2-5] with action

$$S_0 = \frac{1}{2}\int dt\, \mathrm{Tr}\left\{(D_t\Phi)^2 - \Phi^2\right\}, \tag{4.6}$$

with Φ a hermitian matrix.[4] The natural ground state of the fermions in this matrix model is the circular droplet that corresponds to $AdS_5 \times S^5$ on the Type IIB side. Composite operators $\Pi_i(\mathrm{Tr}\,\Phi^{n_i})^{r_i}$ are the natural observables of this matrix model. These observables naturally lead to a multi-parameter family of deformations of the matrix model,

$$S(g_{n_i r_i}) = S_0 + \int dt \sum g_{n_i r_i}\Pi_i(\mathrm{Tr}\ \Phi^{n_i})^{r_i}, \tag{4.7}$$

parametrized by arbitrary coupling constants $g_{n_i r_i}$. In the construction of the corresponding half-BPS Type IIB geometries [1], the matrix model (4.6) with the harmonic oscillator potential does not play any privileged role. All distributions of fermions on the x_1, x_2 appear democratically. Some distributions of fermions will be small perturbations of the $AdS_5 \times S^5$ ground state; those are naturally interpreted as finite-energy excitations of the harmonic oscillator theory (4.6). Other distributions are far from the $AdS_5 \times S^5$ ground state. Our geometry near the topological transition is an example of that. Instead of interpreting such solutions as highly excited state of $AdS_5 \times S^5$, it is more natural to think of them as ground states of a deformed matrix model (4.7). In particular, our topology changing solution, whose Fermi surface is given by (4.5), is naturally interpreted as the ground state of the matrix model with the inverted harmonic oscillator potential,

$$S = \frac{1}{2}\int dt\, \mathrm{Tr}\left\{(D_t\Phi)^2 + \Phi^2\right\}. \tag{4.8}$$

This matrix model captures more naturally the physics of half-BPS perturbations near the ground state of the geometry near topological transition.

[4] For an explanation of how the complex matrix model of the zero modes of $Z = \phi_1 + i\phi_2$ in CFT reduces in the half-BPS sector with $\Delta = J$ to a hermitian matrix model, see [2].

5. Finite N: Topology Change Inside $AdS_5 \times S^5$

Until now we focused on the universal features of the unique topology changing process possible in the LLM geometries, by zooming in on a small neighborhood of the singularity. Now we wish to study the topology changing process embedded into a larger environment, for example, in asymptotic $AdS_5 \times S^5$.

5.1. Topology Change in Asymptotic $AdS_5 \times S^5$

Embedding our topology change into $AdS_5 \times S^5$ requires restoring finite N, and considering a distribution of fermions confined into a compact region in the x_1, x_2 plane. One particularly interesting distribution of fermions with such features is schematically illustrated in Fig. 7. In the p, q coordinates of (4.4), we consider a Fermi surface given by

$$\frac{1}{2}p^2 - \frac{1}{2}q^2 + \frac{g}{4}q^4 = \mu \tag{5.1}$$

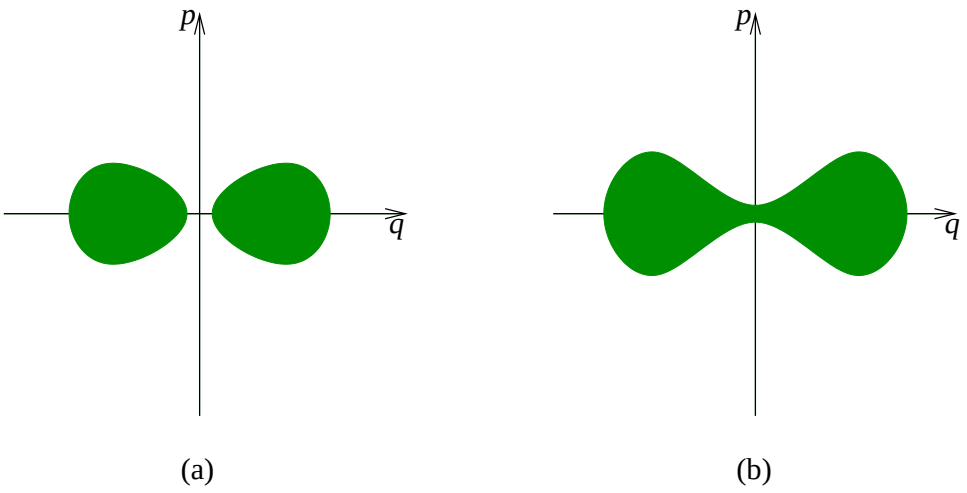

Fig. 7: The topology changing transition inside $AdS_5 \times S^5$. Here (a) corresponds to the Fermi surface (5.1) with $\mu < 0$, and (b) describes $\mu > 0$.

Here μ plays the usual role of a chemical potential for the fermions, with its value determined in terms of N and the quartic coupling constant g by requiring

$$N = \int_{\mathcal{D}} \frac{dp\, dq}{4\pi^2 \ell_p^4}, \tag{5.2}$$

where the integral is performed over the filled droplet(s) $\mathcal{D}$ in the p, q space.

The μ-dependent family of geometries that result from the distribution of fermions with Fermi surface (5.1) describes the macroscopic topology change of half-BPS geometries

asymptotic to $AdS_5 \times S^5$. For $\mu > 0$, we have one connected droplet of fermions, and the topology of the solution is still that of $AdS_5 \times S^5$. However, geometrically, near the origin of AdS_5, the metric of the S^5 factor has been smoothly distorted by fluxes so that its equatorial S^4 is shrinking to zero size. At the point of the topological transition at $\mu = 0$, this S^4 has shrunk to a point precisely at the origin in AdS_5, pinching the original S^5 there into two topologically distinct S^5's. When we continue to $\mu < 0$, these two S^5's will separate, in a process that can be described as the conical singularity of the solution at $\mu = 0$ blowing up into a noncontractible S^4. This noncontractible S^4 can be effectively thought of as the origin of AdS_5 blown up into an S^3, with the remaining angular coordinate on S^4 parametrizing the distance between the two S^5s. Zooming in on the singularity of this solution again reproduces our statement that the spatial slice of the singular solution at infinite N is a cone over $S^4 \times S^4$. This topology change can be viewed as an $AdS_5 \times S^5$ version of anti-de Sitter fragmentation [13].

In the matrix model language, the geometry near its topological transition can be interpreted as a highly excited state in the original matrix model (4.8), or as the ground state of a deformed matrix model (4.7),

$$S(g) = \frac{1}{2} \int dt \, \mathrm{Tr} \left\{ (D_t \Phi)^2 + \Phi^2 - \frac{g}{2} \Phi^4 \right\}. \tag{5.3}$$

related to the original harmonic oscillator model (4.8) by adding two single-trace observables $\mathrm{Tr}(\Phi^2)$ and $\mathrm{Tr}(\Phi^4)$ to the action.

5.2. The Penrose limit as the double scaling limit of noncritical Type 0B theory

It is interesting to take another look at the limit of the $AdS_5 \times S^5$ geometry, near its topological transition, which reproduces the universal geometry studied in Sections 2-4. From the point of view of the asymptotic $AdS_5 \times S^5$ geometry, this involves zooming in on the vicinity of the singularity, and simultaneously scaling μ such that the effective distance between the two components of the Fermi surface stays finite. This can also be seen as an $N \to \infty$ limit, in which we recover the distribution of fermions of Fig. 6.

It turns out that this near-singularity limit has a very natural interpretation, both in supergravity and in CFT.

On the supergravity side, this limit simply corresponds to the Penrose limit. Indeed, notice first that at $\mu = 0$, the singularity itself is a null line in the full ten-dimensional geometry. Moreover, for $\mu \neq 0$, one can mark a point P on the boundary between the filled and empty regions that is near the origin in the p, q coordinates at $y = 0$. In the full geometry, P corresponds to a null geodesic. The Penrose limit towards this geodesic corresponds to shifting the origin of the x_1, x_2 coordinate system to P, rescaling uniformly

$$(x_1, x_2, y) \to \frac{1}{\lambda}(x_1, x_2, y) \tag{5.4}$$

while keeping t constant, and then setting $\lambda = R^2_{AdS} \sim N^{1/2}$ and sending it to infinity. This alone would indeed be the conventional Penrose limit in the LLM coordinates, and would result in the maximally symmetric pp-wave. Here, however, we are interested in a combined limit, which also rescales

$$\mu \to \frac{\mu}{\lambda^2}, \tag{5.5}$$

ensuring that the rescaled distance between the two components of the Fermi surface stays finite as we take the Penrose limit $N \to \infty$. In this way, we stay near the (resolved) singularity during the Penrose limit. The distribution of fermions that corresponds to this Penrose limit of the original $AdS_5 \times S^5$ near its topological transition is that of Fig. 6.

On the CFT side, the double scaling limit (5.4) and (5.5) is precisely the conventional double-scaling limit of the matrix model (5.3)(see e.g. [7] for a review of $c = 1$ strings and the double scaling limit). In this limit, the Φ^4 term in the potential of the matrix model is effectively scaled away, and we are left with the theory of double-scaled fermions in the inverted harmonic oscillator potential – the theory that defines the noncritical $\hat{c} = 1$ Type 0B string theory. After the double scaling limit is taken, the effective string coupling $g_{s,0B}$ of the two-dimensional Type 0B theory is set by the distance between the Fermi surface from the top of the inverted harmonic oscillator potential,

$$g_{s,0B} \sim \frac{1}{\mu}. \tag{5.6}$$

It is pleasing to see that the two natural limits – the Penrose limit in supergravity and the double-scaling limit in the matrix model – are related to each other in this simple way.

Using this relation between the Penrose limit and the double-scaling limit, we expect the scattering amplitudes of the massless tachyon and RR scalar modes of Type 0B string theory in two dimensions to encode the amplitudes for the propagation of half-BPS supergravity modes through our Type IIB solution near its topological transition, i.e., the natural "background S-matrix" observables proposed at the end of Section 3.1.

5.3. Energetics of Topology Change in $AdS_5 \times S^5$

The geometry represented by the Fermi distribution of (5.1) (or Fig. 7) is asymptotically $AdS_5 \times S_5$. However, it does not represent a small perturbation of the $AdS_5 \times S^5$ vacuum. Half-BPS excitations of the vacuum with relatively low energies would be, for example, supergravity modes (with $\Delta \ll N$) or D-branes known as giant gravitons (with $\Delta \sim N$). Our geometry is instead a smooth geometry with fluxes, and cannot be usefully approximated as a distribution of some small number of branes inside $AdS_5 \times S^5$. In fact, using the formula for Δ [1]

$$\Delta = J = \frac{1}{2}\int_{\mathcal{D}} \frac{dp\,dq}{8\pi^3\ell_p^8}(p^2+q^2) - \frac{1}{2}\left(\int_{\mathcal{D}} \frac{dp\,dq}{4\pi^2\ell_p^4}\right)^2 \tag{5.7}$$

one can easily show that our geometry is an excitation of $AdS_5 \times S^5$ with $\Delta \sim N^2$, and therefore represents a qualitatively new effect in $AdS_5 \times S^5$.

Similarly, the Penrose limit of our solution which was the subject of Sections 2-4 is not a low-energy excitation of the pp-wave, i.e., it cannot be obtained from the latter by adding a finite number of supergravity modes or giant gravitons.

Having argued that the generic topology-changing solution in asymptotic $AdS_5 \times S^5$ has $\Delta \sim N^2$, one can ask: what is the *lowest* value of Δ needed for a macroscopic topology change of $AdS_5 \times S^5$, at least within this class of half-BPS geometries? As we will now show, the answer turns out to be of order $\Delta \sim N^{3/2}$. This energy is parametrically lower than the generic value $\Delta \sim N^2$ expexted from a generic smooth LLM geometry, but still higher than $\sim N$, which would result from a small collection of branes/giant gravitons in $AdS_5 \times S^5$.

In the semiclassical fermion picture, this lowest-Δ geometry that changes the topology results from starting with the circular Fermi sea of radius $\sim N$ that describes the vacuum $AdS_5 \times S^5$, and removing $\sim \sqrt{N}$ fermions from it along (say) the $x_2 = 0$ line, thus creating a passage in the Fermi sea of the characteristic width $\sim \sqrt{\hbar}$. Using (5.7) to evaluate Δ for this geometry with the strip removed, we obtain $\Delta \sim N^{3/2}$.[5] In the conventional Type IIB language, this creation of $\sim \sqrt{N}$ aligned holes in the Fermi sea corresponds to placing $\sim \sqrt{N}$ nested giant gravitons on S^5.

6. Other Half-BPS Solutions with Scaling

Until now we focused on the irreducible topology changing process, in which just two components of the Fermi surface meet in a point. As we argued, any other more complicated localized singularity in this class of half-BPS geometries can be smoothly decomposed into a sequence of some number of such irreducible transitions. In the process, the topology of the spacetime changes, at each step by the simple transition described above. Clearly, applying this process many times can lead to fairly complicated topologies, and it would be nice to have a simple tool for analyzing this.

In this section, we present such a tool, in the form of a simple description of all possible localized singularities, irreducible or not, in this class of half-BPS solutions in Type IIB theory. The crucial observation is that the universal features of a localized singularity are captured in the generalized Penrose limit, in which we take the $N \to \infty$ limit and/or zoom in on a small region near the singularity. In that limit, the distribution of fermions

[5] If one were to insist on preserving the overall value of N, the removed fermions would then have to be spread on top of the Fermi surface. It is easy to check that this also causes an effect of order $N^{3/2}$.

that corresponds to the singular geometry will be invariant under uniform rescalings of the x_1, x_2 plane, and consequently, the full solution has to share the same scaling properties (2.12) – (2.15) discussed in Section 2.3.

The corresponding scale-invariant distributions of fermions can be easily classified: they correspond to the Fermi surface consisting of $2k$ straight lines meeting at the origin, with $k = 1, 2, \ldots$, as in Fig. 8.

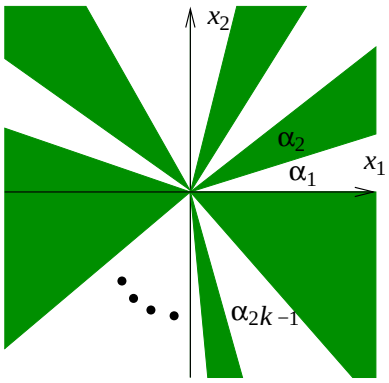

Fig. 8: The fermion distribution that corresponds to a $2k-1$-parameter family of geometries with scaling. This family is parametrized by moduli α_a, $a = 1, \ldots, 2k-1$.

The $2k$ angles α_a between two consecutive (i.e., a-th and $a+1$-st) lines, subject to the constraint that $\sum_{a=1}^{2k} \alpha_a = 2\pi$, represent the moduli of this $2k-1$-parameter family of solutions. The Type IIB geometries of this family can also be easily constructed, by first solving for z with the boundary conditions set by the fermion distribution. Each individual a-th line, with $a = 1, \ldots 2k$, contributes

$$z_a = \frac{v_a}{2\pi\sqrt{v_a^2+y^2}} \arctan\left(\frac{u_a}{v_a^2+y^2}\right) + \frac{v_a}{4\sqrt{v_a^2+y^2}}, \tag{6.1}$$

where

$$\begin{aligned} u_a &= x_1 \cos \sum_{b=1}^{a-1} \alpha_b + x_2 \sin \sum_{b=1}^{a-1} \alpha_b, \\ v_a &= x_2 \cos \sum_{b=1}^{a-1} \alpha_b - x_1 \sin \sum_{b=1}^{a-1} \alpha_b, \end{aligned} \tag{6.2}$$

The total function z for this solution is then

$$z = -\sum_{a=1}^{2k} (-1)^a z_a. \tag{6.3}$$

The full metric and fluxes of this Type IIB solution with a null singularity is then determined in terms of z using the rules summarized in Section 2.1.

The only non-singular geometry on this list is that of $k = 1$, with two lines meeting at the origin at a straight angle, the resulting geometry being the non-singular maximally supersymmetric pp-wave. When the angle between the two lines is $\pi + \alpha$ with α small, the pp-wave solution will develop a mild singularity due to the small localized disturbance of the Fermi sea at the origin. This geometry again has two asymptotic regimes where it is asymptotic to the pp-wave. Introducing observers and coordinates similar to those of Section 3, one can study this perturbed pp-wave as a time-dependent solution, asymptotic to the maximally supersymmetric pp-wave in the far past and the far future. It might be interesting to further study the physics of this perturbation of the pp-wave.

Another interesting geometry in the class studied in this section is the case with $k = 2$, with the four angles given in terms of a small angle α by $\alpha_1 = \alpha_3 = \pi - \alpha$, $\alpha_2 = \alpha_4 = \alpha$, $\alpha \ll 1$. This corresponds to fermions filling the entire plane, with two narrow edges cut out from the Fermi sea in two opposite directions. This geometry is closer to being the (Penrose limit of) the configuration that changes the macroscopic topology of $AdS_5 \times S^5$ at the lowest energy $\Delta \sim N^{3/2}$, as discussed in Section 5.3.

7. Conclusions

In this paper we have initiated the study of spacetime topology change in LLM geometries. We have pointed out that all localized topology changing transitions are reducible to a unique transition, and presented the supersymmetric Type IIB solution that describes the universal features of this unique transition.

We have also shown that this solution can be obtained from a class of topology changing solutions in asymptotic $AdS_5 \times S^5$ as their Penrose limit. On the CFT side, this Penrose limit nicely corresponds to the double scaling limit of the matrix model in an inverted harmonic oscillator potential, which is known to describe noncritical Type 0B string theory in two dimensions.

The spatial section of the solution at topological transition is a cone over $S^4 \times S^4$. The tip of the cone is a supersymmetric, null, point-like singularity. The two ways of resolving the singularity within the half-BPS family closely resemble the conifold transition in Calabi-Yau manifolds.

One fascinating question to ask is whether the singularity can be thermalized. Since this singularity has emerged in the highly controlled class of LLM geometries with sixteen supersymmetries, and the free Fermi theory provides a prescription for the quantization of such geometries, it seems very likely that this singularity should be on the list of "good" spacetime singularities that string theory knows how to make sense of. One general feature expected of "good" singularities in string theory is that they can be thermalized [14] – when we move the solution slightly away from BPS, the singularity turns into a thermal object,

typically carrying macroscopic entropy. In this sense, this thermalization of the singularity is expected to lead to the formation of a macroscopic black-hole horizon. It would be very interesting to study near-BPS versions of our singular geometry, and see whether a finite-area horizon is grown. A natural class of near-BPS states would correspond to the complex matrix model of [2] with both types of oscillators possibly excited, so that the resulting configuration no longer satisfies the BPS condition $\Delta = J$ but the matrix model framework still applies.

Acknowledgements

We wish to thank Mina Aganagic, David Berenstein, Antal Jevicki and Aleksey Mints for useful discussions and comments. One of us (PGS) also benefitted from helpful discussions with Nadir Jeevanjee. This material is based upon work supported in part by NSF grant PHY-0244900, by the Berkeley Center for Theoretical Physics, and by DOE grant DE-AC03-76SF00098. Any opinions, findings, and conclusions or recommendations expressed in this material are those of the author(s) and do not necessarily reflect the views of the National Science Foundation.

References

[1] H. Lin, O. Lunin and J. Maldacena, "Bubbling AdS Space and 1/2 BPS Geometries," hep-th/0409174.

[2] S. Corley, A. Jevicki and S. Ramgoolam, "Exact Correlators of Giant Gravitons from Dual $N = 4$ SYM," hep-th/0111222.

[3] D. Berenstein, "A Toy Model of the AdS/CFT Correspondence," hep-th/0403110.

[4] A. Hashimoto, S. Hirano and N. Itzhaki, "Large Branes in AdS and Their Field Theory Dual," hep-th/0008016.

[5] M.M. Caldarelli and P.J. Silva, "Giant Gravitons in AdS/CFT (I): Matrix Model and Back Reaction," hep-th/0406096.

[6] N. Itzhaki and J. McGreevy, "The Large N Harmonic Oscillator as a String Theory," hep-th/0408180

A. Boyarsky, V.V. Cheianov and O. Ruchayskiy, "Fermions in the Harmonic Potential and String Theory," hep-th/0409129.

[7] I. Klebanov, "String Theory in Two Dimensions," hep-th/9108019

G. Moore and P. Ginsparg, "Lectures on 2D Gravity and 2D String Theory," hep-th/9304011.

[8] M.R. Douglas, I.R. Klebanov, D. Kutasov, J. Maldacena, E. Martinec and N. Seiberg, "A New Hat for the $c = 1$ Matrix Model," hep-th/0307195

T. Takayanagi and N. Toumbas, "A Matrix Model Dual of Type 0B String Theory in Two Dimensions," hep-th/0307083.

[9] D. Ghoshal and C. Vafa, "$c = 1$ String as the Topological Theory on the Conifold," hep-th/9506122.

H. Ooguri and C. Vafa, "Two-Dimensional Black Hole and Singularities of CY Manifolds," hep-th/9511164.

[10] A. Giveon and D. Kutasov, "Little String Theory in a Double Scaling Limit," hep-th/9909110; "Comments on Double Scaled Little String Theory," hep-th/9911039.

[11] R. Dijkgraaf and C. Vafa, "$N = 1$ Supersymmetry, Deconstruction, and Bosonic Gauge Theories," hep-th/0302011.

[12] M. Aganagic, R. Dijkgraaf, A. Klemm, M. Mariño and C. Vafa, "Topological Strings and Integrable Hierarchies," hep-th/0312085.

[13] J. Maldacena, J. Michelson and A. Strominger, "Anti-de Sitter Fragmentation," hep-th/9812073.

[14] S.S. Gubser, "Curvature Singularities: The Good, the Bad, and the Naked," hep-th/0002160.